Chapter 3 Theories

3.1 Principles of Electron Tunneling

The operating principle of STM is based on the quantum mechanical phenomenon of electron tunneling. The concept of the tunneling is interpreted by a one-dimensional model. In classical mechanics, an electron energy E moving in a potential U(z) is describe by

$$\frac{p_z^2}{2m} + U(z) = E, \tag{3.1}$$

where m is the electron mass, 9.1×10^{-28} g. In regions where E>U(z), the electron has a nonzero momentum P_z. On the other hand, the electron cannot penetrate into any region with $E<U(z)$, or a potential barrier. In mechanics, the state of the same electron is described by a wavefunction $\Psi(z)$, which satisfies Schrödinger's equation,

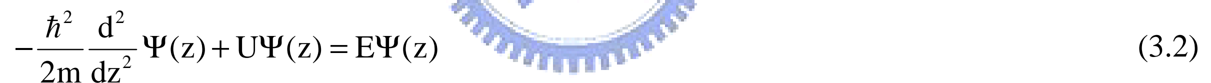

$$-\frac{\hbar^2}{2m}\frac{d^2}{dz^2}\Psi(z) + U\Psi(z) = E\Psi(z) \tag{3.2}$$

Where $\Psi(z)$ is the wave function of the electron.

For an electron with $E = U/2$ incident in a square barrier from the left, as shown in Fig. 3.1. The Schrödinger's equation of this electron

$$-\frac{\hbar^2}{2m}\frac{d^2}{dz^2}\Psi(z) + \frac{1}{2}U\Psi(z) = 0 \tag{3.3}$$

has the solution

$$\Psi(z)=\begin{Bmatrix} Ae^{ikz}+Be^{-ikz}..........(z<0), \\ Ce^{Kz}+De^{-Kz}............(0<z<s), \\ Fe^{ikz}..........................(z>s), \end{Bmatrix} \quad (3.4)$$

where $k=\frac{(2mU)^{1/2}}{\hbar}$; $K=\frac{(mU)^{1/2}}{\hbar}$.

Eq. (3.4) can be solved for the transmission coefficient $T = |F/A|^2$ by matching the boundary conditions on Ψ and $d\Psi/dz$ at $x = 0$ and $x = s$. That is

$$T=\frac{1}{1+(\frac{k^2+K^2}{2Kk})^2\sinh^2 Ks} \quad (3.5)$$

Because the barrier width s is much thicker than the wavefunction decay length $1/K$, $Ks>>1$, the transmission coefficient can be approximated as

$$T\approx\frac{16k^2K^2}{(k^2+K^2)}e^{-2ks} \quad (3.6)$$

It is exponential dependence of the transmission coefficient T on the barrier width s that enables atomic resolution images in tunneling microscopy. It provides a sufficient signal and the tunneling current for atomic scale feedback control of the gap width s along the z direction.

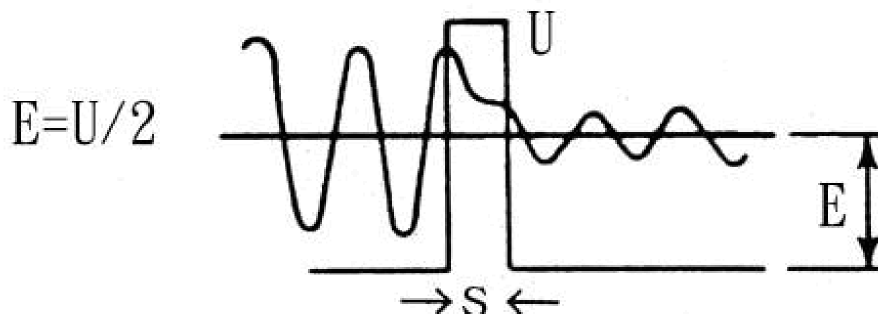

Fig. 3.1 Wavefunction for an election with kinetic energy E=U/2 penetrating a potential barrier U.

3.2 Principles of NC-AFM

3.2.1 Introduction of FM-AFM

NC-AFM is a powerful tool for topographic surface imaging capable of attaining true atomic-scale structures even on insulating surface as well as on conductive surface. The technique can also be used to measure forces in the sub-nN range and has been adapted for investigations of localized charges, magnetic distributions, and contact potentials. In addition to the imaging of surface structure, NC-AFM has also been used for the investigation of local surface properties at a nano-scale resolution. Therefore, we will describe the fundamental principles in NC-AFM in this section.

NC-AFM (also called frequency modulation atomic force microscopy (FM-AFM)) has achieved the long-standing goal of true atomic resolution with AFM in UHV. Our analysis starts with a discussion of the relation between frequency shifts and tip-surface interactions, emphasizing the ability of perturbation theory to describe the measured frequency shift. We discuss the role of short-range chemical interactions in the atomic contrast, with particular attention to semiconductor and ionic (alkali halides and oxides) surfaces. Also included is a detailed quantitative comparison between theoretical simulations and experimentation. Inversion procedures, the determination of the tip-sample interaction from the frequency shift versus distance curves above specific sites, are also reviewed. We finish with a discussion on the optimal range of experimental operation parameters and the use of damping (excitation amplitude) as a source of atomic contrast, including the possible interpretation in terms of microscopic dissipation mechanisms.

The FM mode developed by Albrecht *et al.* provided the key to achieve increased sensitivity through higher quality-factor without any restriction on bandwidth. In the FM mode the signal used to produce the image comes from the direct measurement of the resonance frequency of the cantilever by the tip-surface interaction. In FM-AFM, the spatial

dependence of the frequency shift induced in the cantilever motion by the tip-sample interaction is used as the source of contrast: During the scan, the tip-sample distance is varied in order to achieve a set value for Δf. Thus, the topography in the images represents a map of constant frequency shift over the surface.

In the FM mode (also known as non-contact mode), the cantilever is used as the frequency-determining element of a feedback oscillator. The quantities of experimental interest are Δf, the shift in the resonance frequency of this oscillator under the influence of tip-sample interactions, and A_{exc}, the excitation amplitude of the driving piezo-actuator necessary to maintain the oscillation amplitude of the tip at a pre-set value A. For FM mode is generally used in UHV environment.

3.2.2 Relation between frequency shift and forces

The oscillation frequency is the observable in FM-AFM and it is important to establish a connection between shift and forces acting between tip and sample. While the frequency can be calculated numerically, an analytic calculation is important for finding the functional relationships between operational parameters and the physical tip-sample forces. The motion of the cantilever (spring constant k, effective mass m*, initial potential between tip and sample (V_{ts}) can be described by a weakly disturbed harmonic oscillator. Figure 3.2 shows the deflection $q'(t)$ for the tip of the cantilever. It oscillates with an amplitude A at a distance $q(t)$ from a sample. The closest point to the sample is $q=D$ and $q(t) = q'(t) + d + A$. The Hamiltonian ($\hat{H}$) for the cantilever is

$$\hat{H} = \frac{p^2}{2m^*} + \frac{kq'^2}{2} + V_{ts}(q), \tag{3.7}$$

Where $p = m^* dq'/dt$. The unperturbed motion is given by

$$q'(t) = A\cos(2\pi f_0 t) \qquad (3.8)$$

and the frequency is:

$$f_0 = \frac{1}{2\pi}\sqrt{\frac{k}{m^*}}. \qquad (3.9)$$

If the force gradient $k_{ts} = -\partial F_{ts}/\partial z = \partial^2 V_{ts}/\partial z^2$ is constant during the oscillation cycle, the calculation of the frequency shift is trivial:

$$\Delta f = \frac{f_0}{2k} k_{ts.} \qquad (3.10)$$

However, in classical FM-AFM, varies by several orders of magnitude during one oscillation cycle and a perturbation approach as shown below has to be employed to calculate the frequency shift.

We used the Hamiltion-Jacobi Method to solve these relational equations. The first derivation of the frequency shift in FM-AFM was achieved in (1997) [25] using canonical perturbation theory [26]. The result of this calculation is

$$\Delta f = -\frac{f_0}{kA}\langle F_{ts} q' \rangle = -\frac{f_0^2}{kA^2}\int_0^{1/f_0} F_{ts}[D + A + q'(t)]q'(t)dt. \qquad (3.11)$$

The applicability of first-order perturbation theory depends on the magnitude of the perturbation, i.e. the ratio between V_{ts} and the energy $E = kA^2/2$ of the oscillating cantilever. In FM-AFM, E is typically in the range of several KeV, while V_{ts} is only a few

electron volts. First order perturbation theory yields results for Δf with excellent precision.

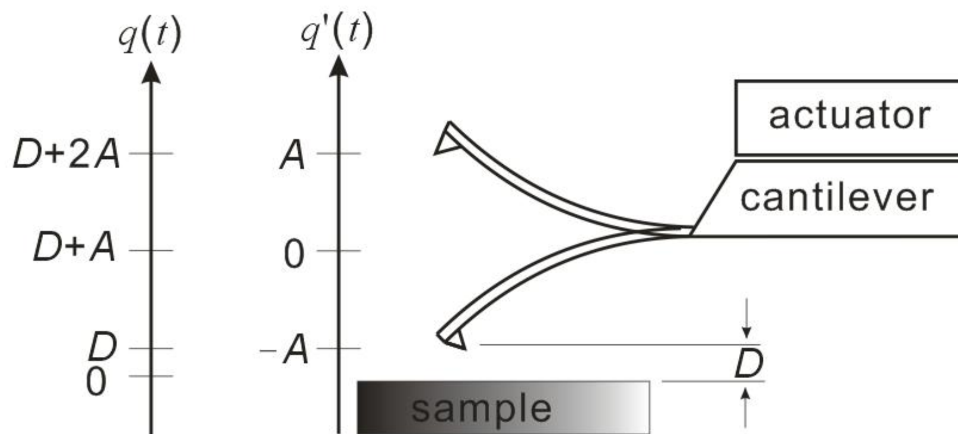

Fig. 3.2 The Schematic view of an oscillating cantilever has definition of geometric terms.

3.3 Interaction Force between the Tip and the Sample

The AFM is similar to a STM, except that a cantilever replaces the tunneling tip. The NC-AFM is based on the detection of forces between the tip and the sample. We can classify the contributions by their range and strength. In vacuum, there are short-range chemical force (fraction of 1 nm), van der Wall force, and electrostatic force with a long range (up to 100 nm).

The total force F_{ts} between tip and sample is composed of several contributions:

$$F_{ts} = F_{chem} + F_{vdW} + F_{el}, \tag{3.12}$$

with the short ranged chemical force, F_{chem} (covalent, ionic, or metallic bonding), the van der Walls force, F_{vdW}, and the long ranged electrostatic force F_{el}.

In regular NC-AFM operation, the electrostatic force is minimized, by applying the correct bias voltage V_t on the tip:

$$F_{el} = -\frac{1}{2}\frac{dC}{dz}U^2 = -\frac{1}{2}\frac{dC}{dz}(V_t + V_{cp})^2 \tag{3.13}$$

Where C, U, V_{cp}, and V_t represents effective capacitance, effective potential difference (EPD), the local contact potential V_{cp} between tip and sample, and the bias voltage on the tip, respectively. The contact potential V_{cp} is the difference in work function between the tip and the sample, that is, $V_{cp} = (\Phi_{tip} - \Phi_{sample})/(-e)$ for conducting tips and samples.

The van der Walls force is independent of V_t and decays faster than the electrostatic force [27]. The plane-sphere interaction force is given by the expression:

$$F_{vdW} = -\frac{HR}{6D^2} \tag{3.14}$$

Where H is the Hamaker constant, R is the tip radius, and D is the tip-sample distance.

The chemical forces are due to developing bonds between tip and sample atoms, and are relevant only at tip-sample distance below ~5 Å [28]. This mechanism is presumably responsible for atomic resolution imaging.

3.4 Calculation of Interaction Force between Tip and Sample

Several groups have obtained images demonstrating true atomic resolution by force microscopy in a noncontact mode (NC-AFM) on different materials. However, proper descriptions of the tip-sample interaction and contrast mechanisms are still under discussion. The extension of NC-AFM beyond topography measurements toward a microscopy of specific surface properties depends very much on an understanding of these issues. Various kinds of interactions, such as van der Waals (vdW), electrostatic, magnetic, and short-range chemical forces, contribute to the total force between the probing tip and sample. These interactions have different distance dependencies. One key problem in NC-AFM is to distinguish and separate these interactions. The characterization of short-range chemical forces is crucial to the understanding of true atomic resolution. The short-range can be developed procedures for single molecule manipulation.

The electrostatic interaction between a tip and a surface has been calculated and been investigated analytically by several authors. Colchero *et al.* describe the cantilever as a tilted plane capacitor and the tip as a charged cone terminated by a parabolic apex [29]. They concluded that the tip apex dominates the tip-sample interaction only for small tip-sample distances below 3-10 nm. Saint Jean *et al.* used a tip model consisting of a cone and a

spherical tip, neglecting the cantilever. They concluded that electrostatic interaction dominates the van der Walls for tip-sample separation larger than half the tip apex radius [30]. Comparing different parameters (apex radius, cone opening angle and cone length) of a tip, Jacobs *et al.* concluded that best resolution in KPFM was achieved for long slender tips with a slightly blunt apex [31]. Olsson *et al.* measured the tip-sample distance as a function of applied bias voltage and compared the shape of the obtained dependence in predictions for different tip models [14], i.e. a sphere, a cone and a parallel plate capacitor opposing a sample surface. These results allow us to acquire information about tip shape based on the data obtained *in situ*.

3.4.1 A tip-lever system

Colchero *et al.* presented an analytical formula for a realistic model for the probe. The tip-lever system is structured with three elemental building blocks: a lever, a tip cone and a tip apex. The lever is characterized by its length l, its width w and an angle θ_{lever} respect to the sample surface. The tip is a truncated cone of height h and opening angle θ_{tip} which ends precisely in a parabolic tip apex of radius R.

For this geometry, the shape and length of the circular segments connecting the probe and the sample can be calculated and relation can be determined to obtain the following forces as a function of the distance between the surface and tip apex:

$$F_{apex} = -\frac{\pi\varepsilon_0 U^2}{1+f(\theta_{tip})(\frac{z}{R})^2}\left(\frac{R+\frac{z}{2}}{R-2z}\right)^2\left(\frac{R-2z}{z[1+2\frac{z}{R}\tan^2(\theta_{tip}/2)]}+2\ln\frac{4z}{2z+R+(R-2z)\cos(\theta_{tip})}\right), \quad (3.15)$$

$$F_{trun_cone} = -\frac{4\pi}{(\pi-\theta_{tip})^2}\varepsilon_0 U^2[\ln\frac{z-\delta/2+h}{z+\delta/2}-\sin(\theta_{tip}/2)\frac{z-\delta}{z-\delta/2+h}\frac{z-\delta/2}{z+\delta/2}], \quad (3.16)$$

$$F_{lever} = \frac{2\tan^2(\theta_{lever}/2)}{\theta_{lever}^2}\varepsilon_0 U^2\frac{lw}{(z+h)^2}\frac{1}{1+2l\tan(\theta_{lever}/2)/(z+h)} \quad (3.17)$$

where $f(\theta_{tip}) = \dfrac{\ln[1/\sin(\theta_{tip}/2)]}{[1-\sin(\theta_{tip}/2)][3+\sin(\theta_{tip}/2)]}$; θ_{tip} is the cone's full opening angle; h is the mesoscopic tip cone of height .

3.4.2 $D(V_t)$

According Eq. (3.11) the F_{ts} is the total force of the tip and the sample:

$$F_{tot}(d) = F_{ts}(d) = F_{vdw} + F_{apex} + F_{cone} + F_{lever}, \qquad (3.18)$$

where $d = D + A + A\cos(2\pi f_0 t)$, d is the instantaneous tip-surface separation, D stands for the nearest position, A represents the cantilever free oscillation amplitude and f_0 the cantilever oscillation frequency. Calculated for f_0 = 260 kHz, Δf = -30 Hz, k= 42 N/m, θ_{tip} = 25°, and H = 4×10^{-19} J, the result was plotted in Fig. 3.3.

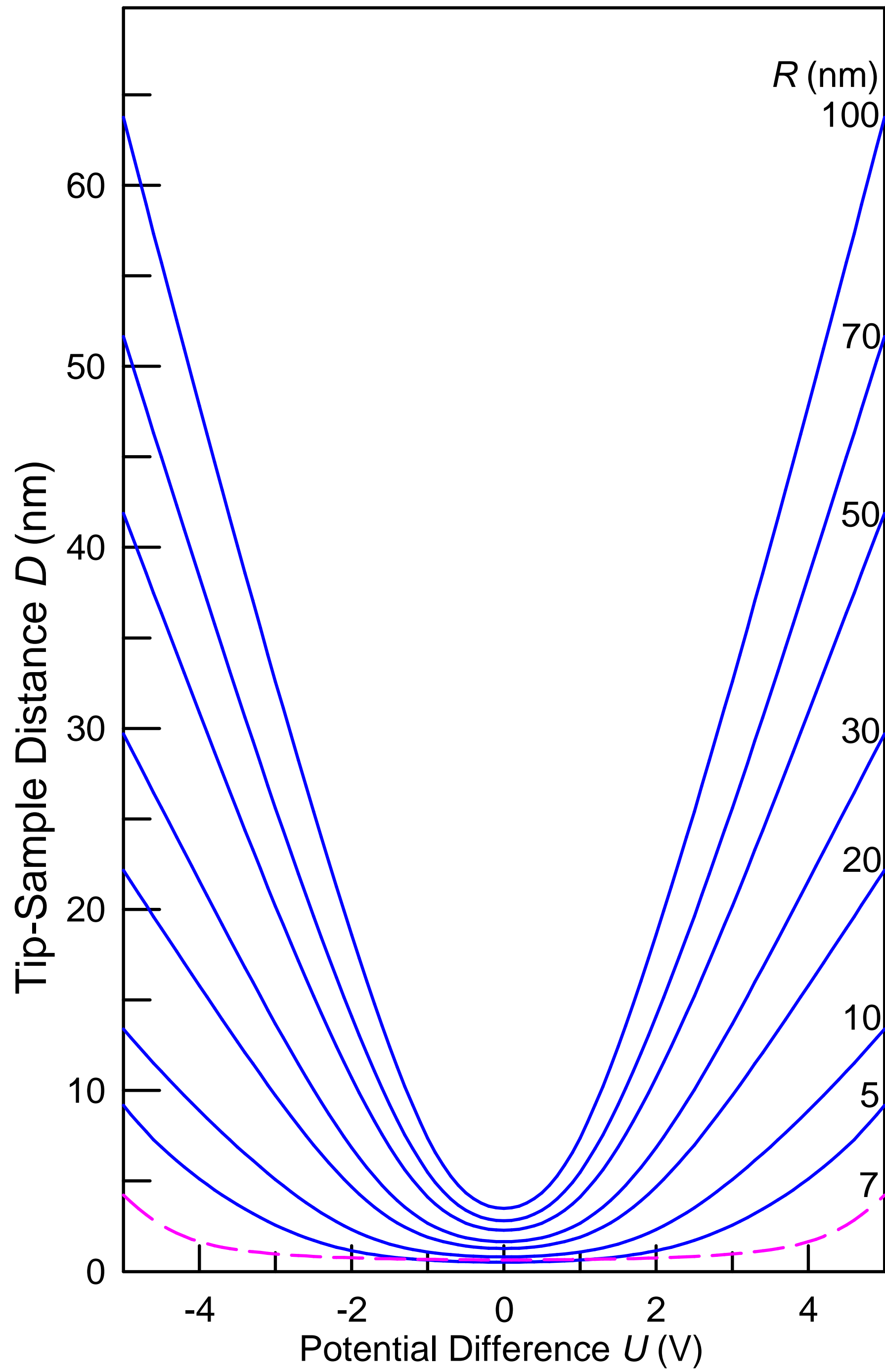

Fig. 3.3 The minimum tip-sample distance D calculated for various tip radii as indicated. The dash curve is calculated by assuming as oxide layer of 7 nm at the tip's end. Parameter: f_0 = 260 kHz, Δf = -30 Hz, k = 42 N/m, Hamaker constant $H = 4\times10^{-19}$ [32], θ_{tip} =25°.